# CLOSED FORM SOLUTION OF AN N-PORT MICROSTRIP PLANAR DISK DEVICE WITH AN ECCENTRICALLY LOCATED SHORT CIRCUIT POST OF ARBITRARY RADIUS

S. R. Judah and M. J. Page

University of Hull, Hull, England. HU4 7RX

## ABSTRACT

**An analysis technique is presented allowing the performance of an N-port microstrip planar disk device with an arbitrarily located internal short circuit (S/C) post of arbitrary radius to be predicted. The approach yields analytical expressions ideal for CAD implementation. The experimental results are in very good agreement with the theoretical predictions.**

## INTRODUCTION

The performance of a multiport planar disk device depends upon the electromagnetic field distribution that occurs within and around the periphery of the device. Any mechanism that enables the peripheral electromagnetic fields to be modified therefore has the potential of becoming an important design tool in the production of planar disk devices.

A technique involving the introduction of a short circuit (S/C) post to multiport planar disk devices has been identified as a means by which the performance of such devices may be modified.

This work presents an analysis technique that allows the performance of a microstrip planar disk device to be predicted when a S/C post of arbitrary radius is positioned anywhere within the periphery of the device. Previous solutions to this problem have used restricting approximations regarding the post radius and post location [1]. These approximations assume a post of very small radius which is well removed from the periphery of the device. In this case the problem is solved without the need for such approximations by making use of the mode matching planar circuit analysis approach [2].

## METHOD OF ANALYSIS

In the mode matching approach the peripheral magnetic and electric fields of the device are represented by Fourier series. Each mode of the Fourier expansion obeys the two-dimensional homogeneous wave equation. The modal expansion coefficients in the series expansion for the fields are then chosen so that the resulting fields satisfy the given source conditions at the boundary.

Consider the circuit of Figure 1 in which the centre of the S/C post is positioned along the $\Phi=0^{\circ}$ axis at the origin of the $\rho,\varphi$ coordinate system.

Fig.1 A Multiport Microstrip Planar Disk Circuit with an Offset S/C Post

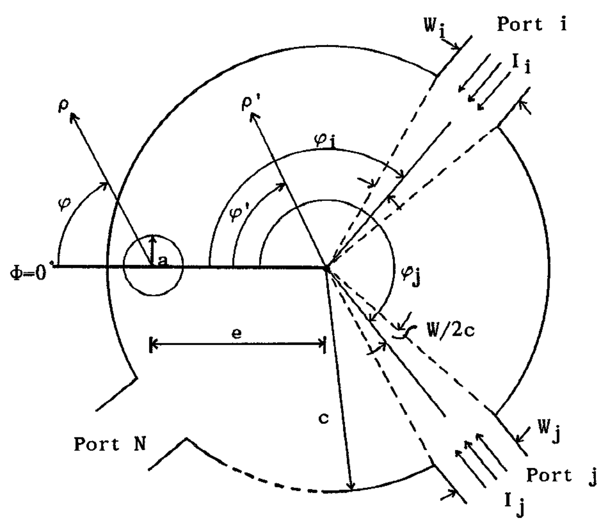


The general solution for the electric field $E_z$ that occurs beneath the N-port device is given by (1).

$$E_z(\rho,\varphi) = \sum_{m=0}^{\infty} (a_m J_m(k\rho) + b_m N_m(k\rho)) \cdot (c_m \cos m\varphi + d_m \sin m\varphi) \quad (1)$$



CH2848-0/90/0000-0371$01.00 © 1990 IEEE

In this expression $J_m(k\rho)$ is the Bessel function of the first kind of order m and $N_m(k\rho)$ is the Bessel function of the second kind of order m. Applying the electric wall boundary condition at $\rho=a$ and shifting from the $\rho,\varphi$ to the $\rho',\varphi'$ coordinate system allows the electric field to be written in terms of $\rho'$ and $\varphi'$.

$$E_z(\rho',\varphi') = \sum_{m=0}^{\infty} A_m \sum_{p=0}^{\infty} \frac{E(m,p,e)}{\epsilon_p} Z_{pm}(k\rho') \cos p\varphi'$$

$$+ \sum_{m=0}^{\infty} B_m \sum_{p=0}^{\infty} F(m,p,e)\, Z_{pm}(k\rho') \sin p\varphi' \quad (2)$$

The term $Z_{pm}(k\rho')$ in (2) is defined by (3)

$$Z_{pm}(k\rho') = \left[ J_p(k\rho') - \frac{J_m(ka)}{N_m(ka)} N_p(k\rho') \right] \quad (3)$$

and $\epsilon_p$ is defined by (4).

$$\epsilon_p = \begin{cases} 2, & p=0 \\ 1, & p\neq 0 \end{cases} \quad (4)$$

The quantities E(m,p,e) and F(m,p,e) are expressed in the form of (5) and (6) respectively. The quantity, e, represents the offset of the centre of the post from the centre of the disk.

$$E(m,p,e) = J_{p-m}(ke) + (-1)^m J_{p+m}(ke) \quad (5)$$

$$F(m,p,e) = J_{p-m}(ke) - (-1)^m J_{p+m}(ke) \quad (6)$$

Using Maxwell's equations it is then possible to derive, from the electric field of (2), the angular magnetic field at the periphery of the disk. This is given by (7).

$$H_\varphi(c,\varphi') = \frac{k}{j\omega\mu_o} \sum_{p=0}^{\infty} \sum_{m=0}^{\infty} A_m \frac{E(m,p,e)}{\epsilon_p} Z'_{pm}(k\rho') \cos p\varphi'$$

$$+ \frac{k}{j\omega\mu_o} \sum_{p=1}^{\infty} \sum_{m=1}^{\infty} B_m\, F(m,p,e)\, Z'_{pm}(k\rho') \sin p\varphi' \quad (7)$$

The term $Z'_{pm}(k\rho')$ in (7) represents the derivative of $Z_{pm}(k\rho')$ with respect to the $\rho'$ coordinate and is defined by (8).

$$Z'_{pm}(k\rho') = \left[ J'_p(k\rho') - \frac{J_m(ka)}{N_m(ka)} N'_p(k\rho') \right] \quad (8)$$

The boundary condition at the periphery of the disk is described by (9).

$$H_\varphi(c,\varphi') = \begin{cases} I_j/W_j, & \varphi_j - W_j/2c < \varphi' < \varphi_j + W_j/2c \\ & j = 1,2 \ldots N \\ 0, & \text{elsewhere} \end{cases} \quad (9)$$

In (9) N represents the number of ports and $I_j$ represents the total current flowing into the device via the $j^{th}$ port. The current per unit width is assumed to be uniform. The quantities $W_j$, $\varphi_j$ and c represent the width of the $j^{th}$ port, the angular displacement of the $j^{th}$ port with respect to the $\Phi=0^\circ$ axis and the disk radius respectively.

The boundary condition of (9) may be represented as the Fourier series of (10)

$$H_\varphi(c,\varphi') = \sum_{p=0}^{\infty} \left[ \frac{a_p}{\epsilon_p} \cos p\varphi' + b_p \sin p\varphi' \right] \quad (10)$$

in which the expansion coefficients $a_p$ and $b_p$ may be expressed in terms of $I_j$, $\varphi_j$ and $W_j$.

It is now necessary to choose the expansion coefficients $A_m$ and $B_m$ in (7) such that (7) and (10) are equivalent. Equating (7) with (10) allows $a_p$ to be expressed as an infinite series involving $A_m$ and $b_p$ to be expressed as an infinite series involving $B_m$. In truncating these series to M terms it is possible, by the use of matrix methods, to express $A_m$ and $B_m$ in terms of $I_j$, $\varphi_j$ and W where it is assumed that $W_i=W_j=W$. Substitution of the resulting expressions for $A_m$ and $B_m$ into the electric field expression of (2) and evaluating the RF potential at the $i^{th}$ port as the average of $E_z d$ over the port width allows the impedance matrix elements of an N-port microstrip planar disk circuit, with an arbitrarily located internal offset S/C post of arbitrary radius, to be written as (11) in which $X_{mn}$ and $Y_{mn}$ are calculable quantities.

When considering a single post, the post is always placed along the $\Phi=0^\circ$ axis. Its arbitrary location is achieved by positioning the coupling ports, including the input port, relative to the $\Phi=0^\circ$ axis.

The scattering matrix representation is obtained using the standard Z-matrix to S-matrix transformation.

$$Z_{ij} = \frac{j\omega\mu_o d}{\pi kc} \sum_{p=0}^{M} \sum_{m=0}^{M} \sum_{n=0}^{M} X_{mn} \cos n\varphi_j \left[ \frac{\sin nW/2c}{nW/2c} \right]$$

$$\cdot (E(m,p,e)/\epsilon_p)\, Z_{pm}(kc) \cos p\varphi_i \left[ \frac{\sin pW/2c}{pW/2c} \right]$$

$$+ \frac{j\omega\mu_o d}{\pi kc} \sum_{p=1}^{M} \sum_{m=1}^{M} \sum_{n=1}^{M} Y_{mn} \sin n\varphi_j \left[ \frac{\sin nW/2c}{nW/2c} \right]$$

$$\cdot F(m,p,e)\, Z_{pm}(kc) \sin p\varphi_i \left[ \frac{\sin pW/2c}{pW/2c} \right] \qquad (11)$$

## RESULTS

Experimental results are compared with the theoretical predictions over the frequency range 2–11 GHz for a 4-port junction of radius 15mm with a post offset of 4mm and post radii of 0.5mm and 5mm. In each case the post is located on the symmetry plane as shown in Figure 2. This post positioning is not a limitation of the analysis and the post may equally well have been placed anywhere within the device. All devices tested were constructed on ULTRALAM 2000 substrate having a thickness of 1.52mm and a relative permittivity of 2.5.

Fig.2 The Location of the S/C Post in the Experimental 4-Port Junction

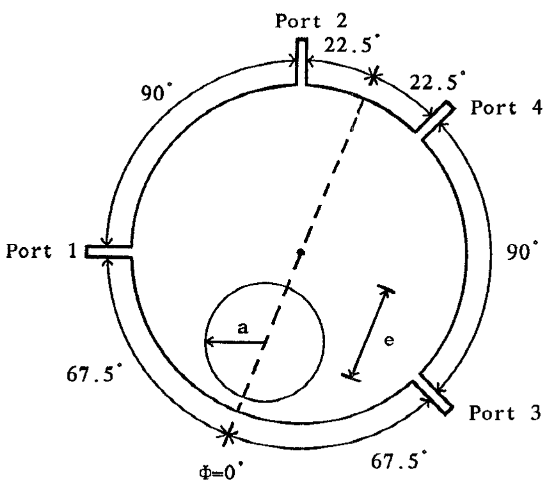


Figures 3a–d compare the theoretical and experimental responses of $|S_{11}|$, $|S_{12}|$, $|S_{13}|$ and $|S_{14}|$ respectively for a 4-port junction having a post radius of 0.5mm with

Fig.3 Theoretical and Experimental Responses for the 4-Port Junction with a 4mm Offset S/C Post of Radius 0.5mm

—— Theoretical - - Experimental

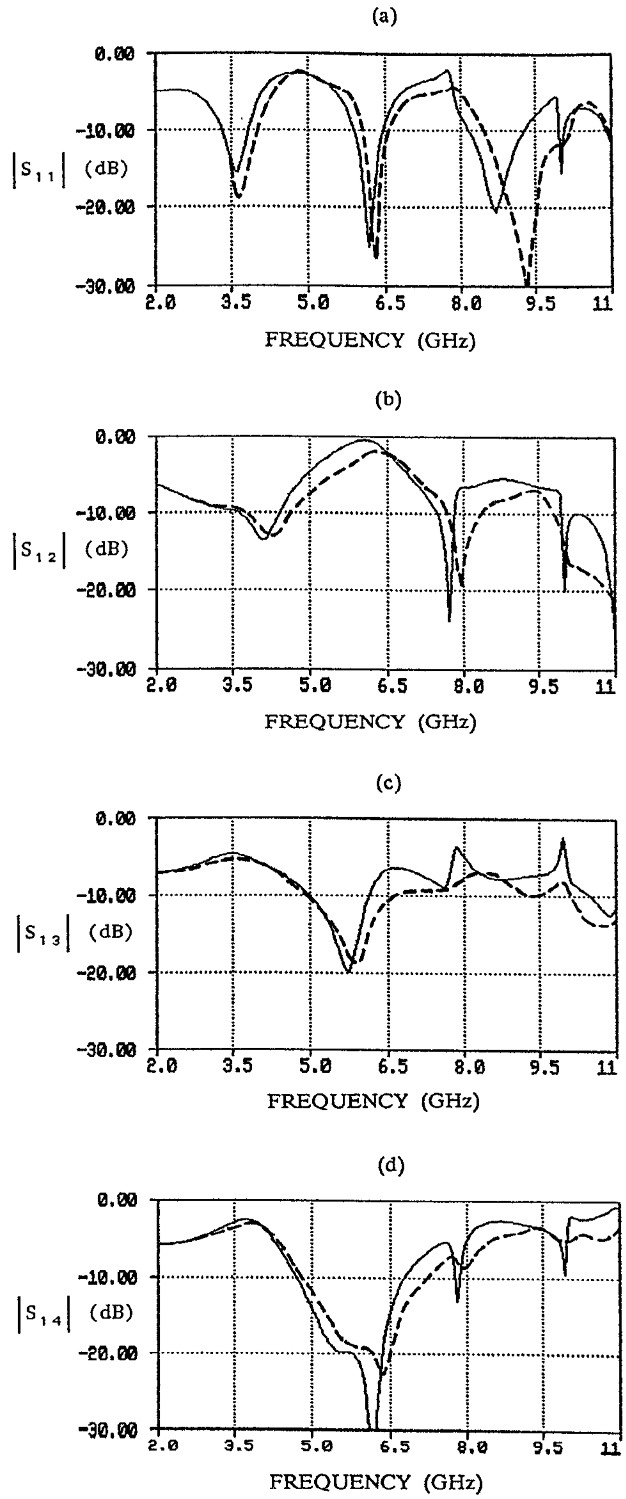

Fig.4 Theoretical and Experimental Responses for the 4-Port Junction with a 4mm Offset S/C Post of Radius 5mm

—— Theoretical - - Experimental

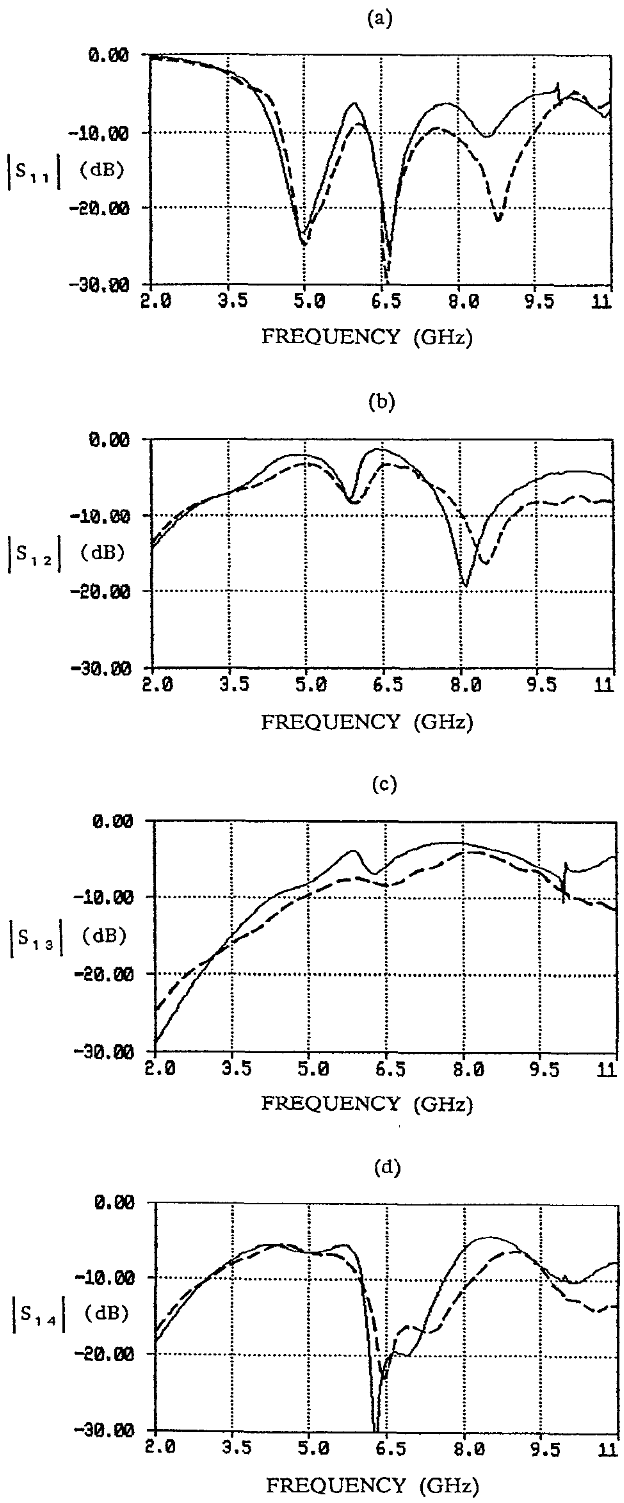


an offset of 4mm. The corresponding results for the 4-port junction having a post of radius 5mm are shown in Figures 4a-d. In both cases the experimental responses show excellent agreement with the theoretical predictions.

An extensive set of experimental results have shown that good agreement with theory is still observed for 4-port junctions of disk radius 15mm with post offsets of 6mm, 8mm, 10mm, 12mm and 14mm.

## V. CONCLUSIONS

The proposed technique allowing the prediction of the response of a multiport microstrip planar disk circuit with a single arbitrarily located offset S/C post of arbitrary radius is verified experimentally. The new technique yields a closed form solution ideal for CAD implementation. The post may be of any radius providing it does not extend beyond the periphery of the disk. The technique presented allows the electromagnetic fields at the periphery of the disk to be altered by the appropriate choice of post size and offset. Since the operation of N-port devices is dependent upon the peripheral fields this technique offers another degree of freedom in the design of planar disk devices.

## ACKNOWLEDGEMENTS

Many thanks are due to John Page, Alan Smith and Rowley Studios for the preparation of device masks and also to John Hodgson and Nigel Mulvana for the manufacture of the devices.

## REFERENCES

1. M. Davidovitz and Y. T. Lo, "Cutoff Wavenumbers and Modes for Annular-Cross-Section Waveguide with Eccentric Inner Conductor of Small Radius", IEEE Trans. Microwave Theory and Tech., Vol. MTT-35, No. 5, May 1987, pp 510-515

2. I. Ohta, I. Hagino and T. Kaneko, "Improved Circular Disk 3 dB Hybrids", Electronics and Comm. in Japan, Part 2, Vol. 70, No.12, 1987, pp 66-77